FEMTOSECOND WHITE-LIGHT LIDAR FOR SIMULTANEOUS CLOUD PARTICLE SIZING AND RELATIVE HUMIDITY MEASUREMENTS

G. Méjean[(1)], R. Bourayou[(2)], J. Kasparian[(1)], M. Rodriguez[(3)], E. Salmon[(1)], J. Yu[(1)], H. Lehmann[(4)], B. Stecklum[(4)], U. Laux[(4)], J. Eislöffel[(4)], A. Scholz[(4)], A. P. Hatzes[(4)], R. Sauerbrey[(2)], L. Wöste[(3)], J. -P. Wolf[(1)]

(1) Teramobile, LASIM, UMR CNRS 5579, Université Claude Bernard Lyon 1, 43 bd du 11 Novembre 1918, F-69622 Villeurbanne Cedex, France, *gmejean@lasim.univ-lyon1.fr*

(2) Teramobile, Institut für Optik und Quantenelektronik, Friedrich-Schiller-Universität Jena, Max-Wien-Platz 1, D-07743 Jena, Germany

(3) Teramobile, Institut für Experimentalphysik, Freie Universität Berlin, Arnimallee 14, D-14195 Berlin, Germany, miguel.rodriguez@physik.fu-berlin.de

(4) Thüringer Landessternwarte Tautenburg (TLS), Karl-Schwarzschild-Observatorium, Sternwarte 5, D - 07778 Tautenburg, Germany), *http://www.tls-tautenburg.de/telesc.html*

ABSTRACT

We use a femtosecond white-light lidar for an extended characterisation of the cloud microphysics. We deduce Particle size and density within the cloud from the multispectral multiple scattering pattern of an ultrashort terawatt laser on a cloud. Furthermore we yield temperature and relative humidity from the spectral analysis of the atmospheric transmission of the white-light continuum from the same laser source which permits to make simultaneous measurements.

1. INTRODUCTION

Cloud nucleation and maturation processes play a key role in atmospheric modeling, both in the meteorological and climatological time and space scales [1]. Their characterization requires continuous measurements of the droplet size distribution within the cloud, with a time resolution in the order of several tens of minutes. The most promising techniques are multispectral or multiple-field-of-view (MultiFOV) Lidars (LIght Detection And Ranging) [2]. These techniques rely on the critical dependence of the Mie scattering efficiency (backscattering and extinction cross sections of the particles) and angular pattern, respectively, with the wavelength and particle size. However these techniques require *a priori* knowledge about the shape of the size distribution as well as the type of the particles themselves. To improve the sensitivity and reliability in the measurements, new remote particle sizing techniques are required.

Besides a full characterization of the cloud microphysics and micrometeorology, *e.g.* droplet growth, requires knowledge about the thermodynamic parameters of the atmosphere, and especially the relative humidity and temperature, with a reasonable vertical resolution.

Ultrashort lasers can efficiently contribute to a better characterization of the cloud microphysics. In the non-linear propagation of Terawatt-femtosecond laser pulses, filamentation [3,4,5,6] generates a white-light continuum extending from the ultraviolet [7,8] to the infrared [9]. This directional, broadband emission provides a basis for white-light Lidar, *i.e.* multispectral Lidar measurements with high spectral resolutions over a bandwidth of several hundreds of nanometers.

Here, we show that the multiple-scattering pattern around the white-light beam impact on the bottom of the cloud can yield a measurement of its droplet size and density. Here, the white-light continuum permits to perform measurements in different spectral regions wide apart from each other, namely the fundamental (800 nm) as well as the blue part of the continuum around 400 nm. The spectral dependence of multiple scattering lifts the ambiguity inherent to fitting with free droplet size and number density. Moreover, high-resolution broadband spectra obtained in the white-light Lidar returns using the same laser source, provide the water vapour mixing ratio (VMR) and temperature of the atmosphere below the cloud layer, which in turn yield the relative humidity of the atmosphere. Although this demonstration was performed in two successive experiments, they use the same laser source and could be driven simultaneously, allowing for a full Lidar characterisation of cloud microphysics.

2. EXPERIMENTAL SET-UP

The experiments reported today have been performed with the mobile femtosecond terawatt laser "*Teramobile*" [10]. This chirped-pulse amplification (CPA) Ti:Sapphire-based laser chain delivered 300 mJ pulses centred at 795 nm at a repetition rate of 10 Hz. For the measurements presented here, the pulses were slightly negatively chirped in the compressor in order to compensate for the atmospheric group velocity dispersion (GVD), leading to an initial pulse duration of 150 fs. The 2 TW output beam was sent collimated with a diameter of 3 cm.

The receiving system consisted of the 2-m primary mirror telescope [11] of the Thüringer Landessternwarte (TLS) observatory, located 30 m away from the laser. The telescope was aimed at the impact of the laser beam on the bottom of the cloud layer, which was imaged on a CCD camera in the Schmidt configuration (FOV 0.6° full angle, 30 times the laser beam diameter). For spectral measurements of the backscattered light, we used the telescope in a Coudé configuration. The signal was analyzed with an Echelle spectrograph [12]. The instrument broadening function has been measured to be Gaussian. All measurements were correlated with the results of an auxiliary, classical Lidar detection providing real-time control of the height and thickness of the clouds.

3. PARTICLE SIZE RETRIEVAL FROM MULTIPLE-SCATTERING PATTERN

Cloud characterization requires the measurement of the droplet number density and size. Recent experiments have shown that clouds or aerosol layers located several km altitude yield valuable signals when imaging backscattered photons, both in the fundamental region and in the blue band of the white-light continuum [13,14] (Fig. 1). Such images bear two types of information. On one hand, differenciating the beam diameter as a function of altitude below the yields the beam divergence, which amounts to 0.16 mrad and 0.5 mrad half width at $1/e^2$ respectively for the fundamental and blue spectral regions. On the other hand, the wide scattering halo on the cloud is a clear signature for strong multiple scattering within it. Once corrected with the parallax induced by the experimental configuration, a cut across this halo provides us with the angular pattern of the multiple scattering, bearing information about the cloud itself.
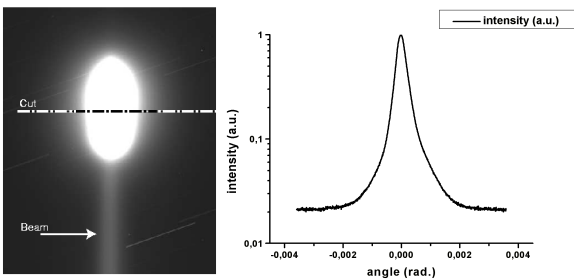

Fig. 1. Beam image observed from the ground in the fundamental region. The lower part of the image (see arrow) corresponds to Rayleigh scattering of the beam below the cloud. The halo is due to multiple scattering in the cloud at 6 km altitude. Multiple scattering patterns are obtained by geometry-corrected cuts across the halo (see dash-dotted line).

High-resolution images of the pattern in two spectral ranges, around 800 nm and 400 nm respectively, provide for the first time a multispectral, multi-field-of-view (multi-FOV) Lidar at this angular resolution. In order to fit the particle size and density within the clouds, we simulated the multiple scattering pattern for given wavelengths, droplet sizes and cloud densities treating the nth-order scattering as n individual scattering event, with an angular probability (treated over 4π sr) given by Mie scattering [15]. Between the scattering events, we considered propagation segments, of length equal to the mean free path of a photon in the cloud. Since we deal with dense clouds in rainy atmospheres, Rayleigh scattering from air molecules is neglected. All calculations are performed assuming a Gaussian incident laser beam, using the divergence measured from the Rayleigh part of the images.
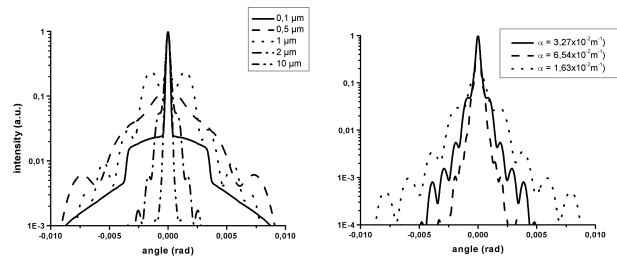

Fig. 2. Simulated angular multiple scattering profiles for clouds composed of 0,1 μm, 0,5 μm, 1,0 μm, 2,0 μm and 10,0 μm water droplets, with an optical density of $3,27 \times 10^{-2}$ m^{-1} and angular multiple scattering profiles for clouds composed of 2 μm water droplets, as a function of the optical density.

Tests within the whole parameter range of interest showed that the orders beyond the 4th-order scattering had a negligible contribution to the scattering pattern (< 5 %). Hence, calculations are restricted to the orders 1 (single scattering) through 3 in the following, reducing the computing time and allowing iterative fitting of the experimental pattern. Since our imaging set-up provides much larger FOV than conventional multiFOV Lidars, we found that an accurate simulation of the multiple scattering pattern in dense clouds can not be restricted to the first forward and backward scattering lobes as *e.g.* in references [16,17], but instead requires to take sideward scattering into account. As shown in Fig. 2, the simulated radial multiple-scattering profile depends critically on the particle size and density within the cloud, allowing a precise determination of the particle size distribution within the cloud.

However the multiple-scattering pattern at only one wavelength does not yield an unambiguous fit. For example, in the case of the data from, two sets of parameters can fit the fundamental pattern: 2 μm radius and a particle density of 7.6×10^8 m^{-3}, or 8 μm and $2,2 \times 10^7$ m^{-3} (Fig. 3). The comparison of the multiple scattering patterns in the blue region shows a significant discrepancy on at larger angles on the pattern. Hence, it permits to select unambiguously the first solution

showing the decisive advantage of using a multispectral analysis. The pretty high cloud density obtained (extinction coefficient of 3.3×10^{-2} m^{-1}) is qualitatively compatible with the intense signal in the auxiliary Lidar detection system.
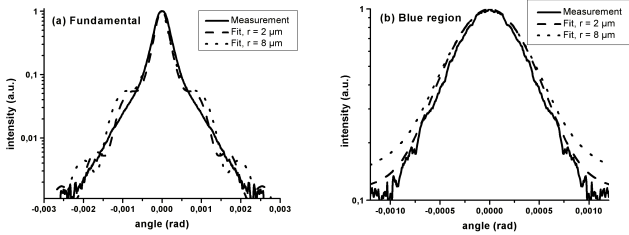

Fig. 3. Experimental and fitted angular distribution of multiple scattering, corresponding to the same data as Erreur! Signet non défini.. The fitting parameters are a cloud density 7.6×10^8 m^{-3} and a droplet radius of 2 μm

4. RELATIVE HUMIDITY RETRIEVAL

Besides the properties of the droplets, a full characterization of the cloud microphysics requires knowledge about the thermodynamical parameters of the atmosphere around it, including relative humidity and temperature. We achieved this measurement with the same laser source as the multiple scattering study for droplet sizing described in the previous section, thus opening the perspective for a simultaneous measurement.

More precisely, we analyzed the spectrum of the white-light continuum spectrum backscattered from clouds located 4.5 km above the ground level, as measured by the auxiliary Lidar. The spectrum of the backscattered white-light was recorded between 680 and 920 nm, thus encompassing the rotational-vibrational band of H_2O centred at 820nm, as well as the O_2 A band around 762 nm. Since the available spectral range covers lines of different intensities, the bands used in the fit have been chosen to optimize the signal while avoiding saturation, related with the actual concentration of the species to be measured. The fits took benefit of the wide available spectral interval. They are based on HITRAN 2000 [18] high-resolution database.

We studied a spectrum acquired at 22 h UT. The temperature was retrieved from the O_2 A band spectrum, and subsequently used to fit the water vapour volume mixing ratio (VMR) of the atmosphere from water absorption. More precisely, the stable meteorological conditions allowed us to consider a standard vertical pressure profile and a typical temperature decrease by 6.5 K/km, and the known VMR of oxygen in the atmosphere (20.9 %) was considered. The retrieved temperature profile is very comparable with the nearest radiosonding temperature profile available (23 h UT, Meiningen, at 100 km distance)

This temperature profile was used as reference in the analysis of the water vapour 4ν-overtone band in both the 813-816 nm and in the 825-829 nm region (Fig. 4.), yielding a relative humidity of (49±3) %, in good agreement with the vertical average of the radiosonde data. Hence, white-light Lidar data have, for the first time, allowed multicomponent measurements yielding both temperature profile and relative humidity data, which are key parameters in understanding the physics of cloud formation and precipitation.
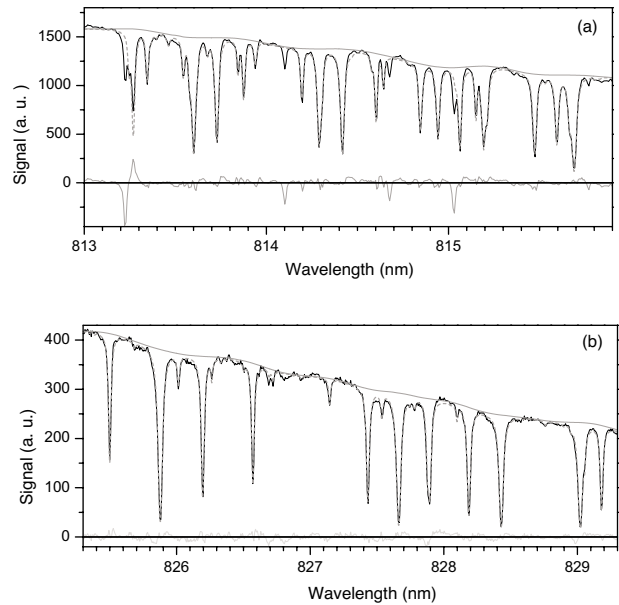

Fig. 4. Fit of the water absorption spectrum in the 4ν-overtone band in the 813-816 nm (a) and 825-829 nm (b) regions. Black solid line: measurement; grey dotted line: fit; grey solid line near zero: residuum of the fit. The smooth line is the estimation of the background. Note that the extremely long absorption path allows to measure weak lines not tabulated in the HITRAN 2000 database.

Spectral measurements thus simultaneously yielded the temperature and relative humidity of the air mass under the clouds, within an error compatible with the requirements of meteorological or climatological modeling purposes. Two variants have been used, in which multiple parameters are retrieved either from distinct spectral regions, or from one single, broad wavelength interval. Moreover, in the Lidar configuration used for this experiment, a differentiation of the backscattered white-light with respect to altitude would yield altitude-resolved relative humidity profiles, therefore allowing for humidity mapping across the atmosphere.

5. CONCLUSION

As a conclusion, the supercontinuum generated through the filamentation of femtosecond pulses during their

vertical propagation in the atmosphere was used to characterize both the clouds (droplet size and number density) and the thermodynamical properties of the atmosphere in their vicinity, such as the temperature and relative humidity. Since both of these measurements use the same laser source equipped with diagnostics for imaging and spectral analysis, they are suitable for a simultaneous operation, opening the way to a full characterization of the cloud microphysics by combined white-light differential absorption and multispectral multiFOV Lidar. This type of data is of high relevance for atmospheric modelling, especially considering the 2D and 3D mapping capability of Lidar. Moreover, using more than two spectral regions, and reducing the filter bandwidths, may allow to remotely measure not only the mean size, but also size distribution and shape of the droplets within the clouds.

1. Pruppacher H. R. and Klett J. D., *Microphysics of clouds and precipitation*, Riedel Publishing Company, Dordrecht (Nethernalnds), 1978

2. R. M. Measures, *Laser Remote Sensing – Fundamental and Applications*, Wiley Interscience, New York, 1984.

3. Braun A., et al. Self-channeling of high-peak-power femtosecond laser pulses in air, Optics letters **20**, 73 (1995)

4. Nibbering E. T. J., et al. Conical emission from self-guided femtosecond pulses in air, Optics letters **21**, 62 (1996).

5. Brodeur A., et al. Moving focus in the propagation of ultrashort laser pulses in air, Optics Letters **22**, 304 (1997)

6. Mlejnek M., et al. Dynamic spatial replenishmentof femtosecond pulses propagating in air, Optics Letters **23**, 382 (1998)

7. Aközbek N., et al. Third-Harmonic Generation and Self-Channeling in Air Using High-Power Femtosecond Laser Pulses, Physical Review Letters **89**, 143901 (2002)

8. Méjean G. et al. UV-Supercontinuum Generated by Kilometer-Range Filamentation in Air, (in preparation)

9. Kasparian J., et al. Infrared extension of the hypercontinuum generated by fs-TW-laser pulses propagating in the atmosphere, Optics Letters **25**, 1397 (2000)

10. Wille H., et al. Teramobile: a mobile femtosecond-terawatt laser and detection system, European Physical Journal - Applied Physics **20**, 183 (2002)

11. Lehmann H., The 2m telescope, (2002), http://www.tls-tautenburg.de/telesc.html

12. Lehmann H., Coudé Echelle Spectrograph, (2002), http://www.tls-tautenburg.de/coude/echelle_spectrograph.html

13. Rodriguez M., et al. Kilometer-range non-linear propagation of fs laser pulses, to be published in Physical Review E (2004)

14. Kasparian J., et al. White-Light Filaments for Atmospheric Analysis, Science **30**1, 61 (2003)

15. Toon O. B. and Ackerman T. P., Algorithms for the calculation of scattering by stratified spheres, Applied Optics **20**, 3657-3660 (1981)

16. Pal S. R. and Carswell A. I., Multiple scattering in atmospheric clouds: lidar observations,Applied Optics **1**5, 1990-1995 (1976)

17. Bissonnette L. R., Multiple-scattering Lidar equation, Applied Optics **3**5, 6449 (1996)

18. Rothman L. S., et al. "The HITRAN Molecular Spectroscopic Database: Edition of 2000 Including Updates of 2001", Journal of quantitative spectroscopy and radiation transfer **82**, in press (2003)